molecular pharmaceutics

Article

pubs.acs.org/molecularpharmaceutics

Fatty Acid-Binding Protein 5 Facilitates the Blood–Brain Barrier Transport of Docosahexaenoic Acid

Yijun Pan,[†] Martin J. Scanlon,[‡] Yuji Owada,[§,⊥] Yui Yamamoto,[§] Christopher J. H. Porter,[†] and Joseph A. Nicolazzo*[,†]

[†]Drug Delivery, Disposition and Dynamics, Monash Institute of Pharmaceutical Sciences and [‡]Medicinal Chemistry, Monash Institute of Pharmaceutical Sciences, Monash University, 399 Royal Parade, Parkville, Victoria 3052, Australia

[§]Department of Organ Anatomy, Yamaguchi University Graduate School of Medicine, Minami-kogushi 1-1-1, Ube 755-8505, Japan

[⊥]Department of Organ Anatomy, Tohoku University Graduate School of Medicine, Seiryo-machi 2-1, Aoba-ku, Sendai 980-8575, Japan

Supporting Information

ABSTRACT: The brain has a limited ability to synthesize the essential polyunsaturated fatty acid (PUFA) docosahexaenoic acid (DHA) from its omega-3 fatty acid precursors. Therefore, to maintain brain concentrations of this PUFA at physiological levels, plasma-derived DHA must be transported across the blood–brain barrier (BBB). While DHA is able to partition into the luminal membrane of brain endothelial cells, its low aqueous solubility likely limits its cytosolic transfer to the abluminal membrane, necessitating the requirement of an intracellular carrier protein to facilitate trafficking of this PUFA across the BBB. As the intracellular carrier protein fatty acid-binding protein 5 (FABP5) is expressed at the human BBB, the current study assessed the putative role of FABP5 in the brain endothelial cell uptake and BBB transport of DHA *in vitro* and *in vivo*, respectively. hFAPB5 was recombinantly expressed and purified from *Escherichia coli* C41(DE3) cells and the binding affinity of DHA to hFABP5 assessed using isothermal titration calorimetry. The impact of FABP5 siRNA on uptake of ^{14}C-DHA into immortalized human brain microvascular endothelial (hCMEC/D3) cells was assessed. An *in situ* transcardiac perfusion method was optimized in C57BL/6 mice and subsequently used to compare the BBB influx rate (K_{in}) of ^{14}C-DHA between FABP5-deficient (FABP5$^{-/-}$) and wild-type (FABP5$^{+/+}$) C57BL/6 mice. DHA bound to hFABP5 with an equilibrium dissociation constant of 155 ± 8 nM (mean ± SEM). FABP5 siRNA transfection decreased hCMEC/D3 mRNA and protein expression of FABP5 by 53.2 ± 5.5% and 44.8 ± 13.7%, respectively, which was associated with a 14.1 ± 2.7% reduction in ^{14}C-DHA cellular uptake. By using optimized conditions for the *in situ* transcardiac perfusion (a 1 min preperfusion (10 mL/min) followed by perfusion of ^{14}C-DHA (1 min)), the K_{in} of ^{14}C-DHA was 0.04 ± 0.01 mL/g/s. Relative to FABP5$^{+/+}$ mice, the K_{in} of ^{14}C-DHA decreased 36.7 ± 12.4% in FABP5$^{-/-}$ mice. This study demonstrates that FABP5 binds to DHA and is involved in the brain endothelial cell uptake and subsequent BBB transport of DHA, confirming the importance of this cytoplasmic carrier protein in the CNS exposure of this PUFA essential for neuronal function.

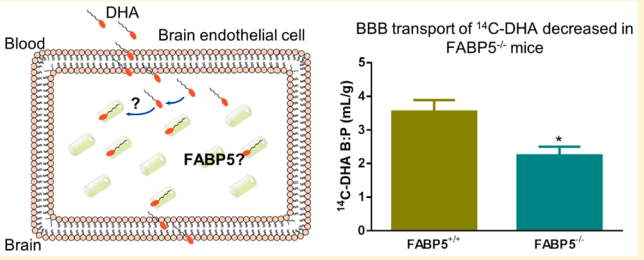

KEYWORDS: *blood–brain barrier, docosahexaenoic acid, fatty acid-binding protein, hCMEC/D3 cells, intracellular trafficking*

INTRODUCTION

Docosahexaenoic acid (DHA) is an essential polyunsaturated fatty acid (PUFA) and is well recognized as having beneficial effects on cognitive function and memory.[1] DHA is sufficiently important to brain function in that an alteration in brain levels of DHA has been found to be associated with neurodegenerative diseases such as Alzheimer's disease.[2−4] The brain has a limited ability to synthesize DHA from its omega-3 fatty acid precursors, and the majority of the DHA that is required for neuronal function is derived from the plasma. Blood-borne DHA must therefore traverse the blood–brain barrier (BBB) to reach the brain.[5,6] Characterization of the molecular factors that govern BBB transport of DHA may therefore assist the development of new treatments to modify brain DHA levels in diseases where the concentrations of this PUFA are affected.

The BBB is composed of a single layer of specialized microvascular endothelial cells that are joined by interendothelial tight junctions, severely limiting paracellular permeability. As such, transcellular transport is the only means by which molecules can traverse a healthy BBB.[7] The mechanism by which PUFAs (such as DHA) are transported across the BBB has been the subject of much investigation, with both

Received: July 22, 2015
Revised: October 6, 2015
Accepted: October 12, 2015
Published: October 12, 2015

DOI: 10.1021/acs.molpharmaceut.5b00580
Mol. Pharmaceutics 2015, 12, 4375−4385

passive diffusion and carrier-mediated transport being implicated.[8−10] In support of passive diffusion as the primary route of DHA transport, *in situ* transcardiac perfusion studies have demonstrated that the BBB transport of ^{14}C-DHA is unaffected by increasing concentrations of unlabeled DHA, consistent with a nonsaturable process.[10] In contrast, others have demonstrated the involvement of membrane transporters, such as fatty acid transport protein-1 and 4 (FATP-1/4) and FAT/CD36 in the BBB transport of PUFAs.[8] Whether FATP-1/4 and FAT/CD36 facilitate DHA transport across the BBB has not been investigated; however, this is possible given that they are expressed at the BBB and DHA is a potential substrate.[11] More recently, the orphan transporter Mfsd2a has also been shown to be a major contributor to the BBB transport of lysophosphatidylcholine (LPC)-DHA, with BBB transport of LPC-DHA being reduced by 90% in Mfsd2a-deficient mice.[9]

Regardless of whether DHA permeates the luminal membrane of brain endothelial cells via passive or active transport, the mechanism of transport of such a poorly water-soluble PUFA through the aqueous intracellular environment from the luminal to abluminal membrane remains to be characterized. The aqueous solubility of long-chain fatty acids (such as DHA) is extremely low (1−10 nM),[12] and a cytoplasmic binding protein may therefore be required to facilitate their trafficking across the aqueous cytoplasm. In other biological locations, lipid-binding proteins traffic fatty acids within the intracellular environment.[13] One such member of the intracellular lipid binding protein family is fatty acid-binding protein (FABP), of which there are nine isoforms. FABPs are highly expressed in almost all tissues with high rates of fatty acid uptake and lipid metabolism.[14] FABPs present two small α-helices connected by a loop, forming a portal region. The interior of the protein contains a large cavity, partially filled with ordered water molecules, that serves as a binding pocket for the ligand.[16] It is believed that the net positive charge of the portal region leads to the formation of a collisional complex with the negatively charged cell membrane.[17−19] The FABP-membrane interactions may therefore catalyze the conformational change of the portal region, thus promoting fatty acid binding or release.[19] FABPs transfer their ligands by direct interaction with the luminal membrane, with the exception of FABP1.[16,20]

The brain endothelial cells lining the cerebral microvasculature (i.e., the BBB) have been reported to express primarily FABP5.[8] Our laboratory recently conducted a genetic screen for FABP isoforms in immortalized human brain microvascular endothelial (hCMEC/D3) cells. In line with Mitchell et al., we not only detected mRNA and protein expression of FABP5, but also detected the presence of FABP3 and FABP4.[15] Although there are no reports of a functional role of FABP3 and 4 at the BBB, FABP5 has been shown to facilitate the *in vitro* BBB transport of palmitic, oleic, and linoleic acid, with genetic silencing of FABP5 leading to a dramatic reduction in the transport of these fatty acids across a monolayer of primary human brain endothelial cells.[8] In these published studies, the involvement of FABP5 in fatty acid transport across the BBB was not explored *in vivo*, and the role of FABP5 in DHA transport was not assessed. Whether FABP5 facilitates brain endothelial cell uptake of DHA and subsequent BBB transport *in vivo* therefore remains unexplored.

In light of previous studies suggesting a role of FABPs in fatty acid transport across the BBB and given that FABP5 appears to be more specific for long-chain fatty acids, regardless of the degree of unsaturation,[8] the current study explored the involvement of FABP5 in the BBB transport of DHA. Human recombinant FABP5 (hFABP5) was expressed in *Escherichia coli* and purified using fast protein liquid chromatography. The binding affinity of the purified hFABP5 to DHA was measured using isothermal titration calorimetry, and the functional role of FABP5 in BBB transport of DHA was studied *in vitro* using hCMEC/D3 cells (in the presence and absence of FABP5 gene silencing) and *in vivo* by performing *in situ* transcardiac perfusions in FABP5-deficient (FABP5$^{-/-}$) and wild type (FABP5$^{+/+}$) mice. The *in situ* transcardiac perfusion technique was modified and validated prior to application in this study.

MATERIALS AND METHODS

Materials. OverExpress *E. coli* C41 (DE3) competent cells, EDTA-free protease inhibitor cocktail tablets, and DHA were purchased from Lucigen (Middleton, WI), Roche Diagnostics GmbH (Mannheim, Germany), and Cayman Chemicals (Ann Arbor, MI), respectively. EGM-2 Endothelial Cell Growth Medium-2 BulletKit was obtained from Lonza (Walkersville, MD), and hFABP5 ELISA kit was purchased from DL Sci&Tech Development (Wuxi, Jiangsu, China). iScript One-Step RT-PCR Kit was obtained from Bio-Rad (Hercules, CA). Isopropyl ß-D-1-thiogalactopyranoside (IPTG) was purchased from Astral Scientific (Caringbah, New South Wales, Australia), and yeast extract and tryptone were purchased from Oxoid (Basingstoke, UK). Columns for protein purification including HisTrap HP 5 mL, HiTrap Phenyl HP 5 mL, and HiPrep 26/10 desalting columns were purchased from GE Healthcare (Piscataway, NJ). Rabbit anti-FABP5 polyclonal antibody and goat antirabbit IRDye 800CW secondary antibody were sourced from Abcam (Cambridge, MA) and Licor Biosciences (Lincoln, NE), respectively. HiPerfect transfection reagent, hFABP5 FlexiTube siRNA (SI03145835), and RNeasy Plus mini kit were purchased from Qiagen (Hilden, Germany). Hydrogen peroxide (30% w/v), Taqman primer/probe for human FABP5 (Hs02339439_g1, FAM) and GAPDH (Hs0227258991_g1, FAM), and Pierce BCA protein assay kit were obtained from Life Technologies (Rockford, IL). The radioactive probes ^{14}C-sucrose, ^{3}H-diazepam, and ^{14}C-DHA were purchased from American Radiolabeled Chemicals, Inc. (St. Louis, MO). Solvable, Ultima Gold liquid scintillation cocktail, scintillation vials, and ^{14}C-glucose were obtained from PerkinElmer Life Sciences (Waltham, MA). Kanamycin sulfate and 4-(2-hydroxyethyl)-1-piperazineethanesulfonic acid (HEPES) were purchased from Amresco (Solon, OH). EMSURE ACS sodium chloride and ammonium sulfate were purchased from Merck KGaA (Darmstadt, Germany). Phenylmethylsulfonyl fluoride (PMSF), imidazole, 1-butanol, phloretin, penicillin−streptomycin, rat tail collagen type I, Hank's balanced salt solution (HBSS), Dulbecco's phosphate buffered saline (D-PBS), Tween 20, agar, formic acid, acetonitrile, 2.5% trypsin, Triton X-100, and sodium deoxycholate were all purchased from Sigma-Aldrich (St. Louis, MO). All chemicals used were of analytical grade, and water was obtained from a Milli-Q water purification system (Millipore, Bedford, MA).

Expression and Purification of Human FABP5. Plasmid pET-28a (+) vectors containing hFABP5 with a kanamycin-resistance gene were generated by cloning between the 5′ Nco I and 3′ BamH I sites (prepared by DHA 2.0, Menlo Park, CA). *E. coli* C41 (DE3) cells were transformed with these plasmids

DOI: 10.1021/acs.molpharmaceut.5b00580
Mol. Pharmaceutics 2015, 12, 4375−4385

using the heat shock method.[21] Transformed cells were grown in Luria−Bertani media containing kanamycin (50 μg/mL) at 37 °C until the optical density at 600 nm reached 0.6, when the culture was induced with 1 mM IPTG. The expression culture was incubated for 6 h postinduction at 37 °C and harvested by centrifugation (4000*g* for 20 min at 4 °C). The cell pellet was resuspended and lysed by sonication in a buffer (25 mM HEPES pH 8, 250 mM NaCl, and 5 mM imidazole) containing EDTA−free protease inhibitor cocktail and 1 mM PMSF. hFABP5 was purified by nickel metal affinity chromatography (HisTrap column) using an elution gradient of 0−0.5 M imidazole and was further purified by hydrophobic interaction chromatography by saturating the fraction containing hFABP5 with 2 M ammonium sulfate and loading the resulting soluble fraction onto a HiTrap Phenyl HP 5 mL column. Protein was eluted using a gradient from 2 to 0 M ammonium sulfate over six column volumes. The hFABP5-containing fraction was treated with tobacco etch virus protease at 4 °C overnight to cleave the N-terminal His-tag, which was removed by passing the sample through a HisTrap column. hFABP5 was delipidated by mixing with 1-butanol (1:1 v/v), and 1-butanol was subsequently separated by centrifugation, and the protein was buffer exchanged into storage buffer (HEPES 20 mM pH 8 and NaCl 50 mM). The hFABP5-containing fraction was confirmed by SDS-PAGE with a Coomassie blue stain. The purified protein was concentrated by ultrafiltration on an Amicon stirred cell (3 kDa cutoff regenerated cellulose membrane, Millipore, Sydney, New South Wales, Australia) to 10 mg/mL, with the protein concentration estimated using a NanoVue (GE Healthcare, Piscataway, NJ). The extinction coefficient for hFABP5 was calculated from the amino acid composition using ExPASy (http://au.expasy.org/tools/protparam.html).

Protein Characterization. The purity of hFABP5 was assessed by SDS-PAGE, and gels were either Coomassie blue stained or analyzed by Western blotting. For Western blotting, hFABP5 was detected using a rabbit polyclonal antibody (1:500 dilution) and goat antirabbit IRDye 800CW secondary antibody (1:7500 v/v dilution) and imaged using a Licor Odyssey scanner (Lincoln, NE) following electrophoresis. To determine the molecular weight, the purified hFABP5 was loaded onto a Shimadzu LCMS-2020 (Canby, OR) coupled with a Luna HPLC C_8 column (Phenomenex, Torrance, CA) with solvent A containing 0.1% v/v formic acid in water and solvent B containing 80% v/v acetonitrile and 0.1% v/v formic acid in water. The flow rate was set at 0.2 mL/min, and the solvent B% was increased from 0 to 60% over 10 min.

Isothermal Titration Calorimetry. The affinity of DHA for hFABP5 was measured in a MicroCal iTC_{200} (GE Healthcare, Piscataway, NJ). The syringe was filled with hFABP5 (0.1 mM in storage buffer), and the sample cell was filled with 0.01 mM DHA in the same storage buffer. The sample cell and the syringe were first equilibrated to 25 °C followed by an initial delay of 180 s before the first injection. In all experiments, a total of 20 injections were performed with a spacing of 260 s. For each injection, a 2 μL volume of hFABP5 solution was introduced into the cell over a duration of 4 s with the syringe stirring continuously in the sample cell at 800 rpm. A blank titration (i.e., blank storage buffer in the sample cell) was performed to determine the background heat of dilution. The binding data were analyzed using the Origin 7.0 software. A one site binding model was fit to the data to calculate binding parameters including the equilibrium dissociation constant (K_D) and experimental number of binding sites (N).

Cell Culture. The hCMEC/D3 cell line was obtained from Pierre-Olivier Couraud (INSERM, France). Cells were maintained at 37 °C in a humidified incubator (5% CO_2/95% O_2) in endothelial basal medium-2 supplemented with vascular endothelial growth factor (0.025% v/v), insulin-like growth factor 1 (0.025% v/v), epidermal growth factor (0.025% v/v), basic fibroblast growth factor (0.1% v/v), hydrocortisone (0.01% v/v), ascorbic acid (0.01% v/v), fetal bovine serum (0.1% v/v), HEPES (1M, pH 7.4, 1% v/v), and penicillin−streptomycin (1% v/v). The cells were seeded at 50 000 cells/cm^2 onto culture flasks/plates coated with rat tail collagen type I. Culture medium was changed every 2−3 days until cells reached a confluent monolayer.

siRNA Transfection. siRNA complexes (5 nM; containing the siRNA target sequence 5′-AGGAGTTAATTA-AGAGAATGA-3′) were added to hCMEC/D3 cells 4−6 h after seeding onto collagen coated plates. siRNA complexes were formed by mixing siRNA with HiPerFect Reagent and incubating for 10 min at room temperature. Cells were incubated with these complexes at 37 °C for 48 h at 5% CO_2/95% O_2. After this initial 48 h, the media was removed and fresh media containing siRNA complexes added, and cells incubated for an additional 48 h. To ensure the transfection did not affect gross morphology, hCMEC/D3 cells were assessed visually after the 96-h incubation using phase contrast microscopy (Nikon, Tokyo, Japan).

mRNA Expression of FABP5 in hCMEC/D3 Cells. Total RNA from mock and siRNA transfected hCMEC/D3 cells was isolated using an RNeasy Plus Mini Kit (Qiagen). Each PCR reaction mixture (25 μL) contained 12.5 μL of iScript 2X probes RT-PCR reaction mix, 0.5 μL of iScript reverse transcriptase, 0.695 μL of Taqman primer/probe, 100 ng of RNA (in 5 μL), and 6.305 μL of nuclease-free water. Measurement of gene expression by quantitative analysis was carried out in a CFX96 system (Bio-Rad, Hercules, CA). Thermocycling was performed at 50 °C for 10 min, 95 °C for 5 min, followed by 50 cycles of 95 °C for 15 s and 60 °C for 30 s. The threshold cycles (C_t) were calculated automatically using the CFX manager software. To determine relative gene expression between mock and FABP5 siRNA transfected cells, the fold-change method ($2^{-\Delta\Delta Ct}$) was employed using eqs 1 and 2, with GAPDH used as a housekeeping gene:

$$\Delta C_t = C_{t(\text{FABP5})} - C_{t(\text{GAPDH})} \quad (1)$$

$$\Delta\Delta C_t = \Delta C_{t(\text{siRNA transfected cells})} - \Delta C_{t(\text{mock cells})} \quad (2)$$

Protein Expression of FABP5 in hCMEC/D3 Cells. A commercially available sandwich hFABP5 ELISA kit (containing an antibody targeting hFABP5, hFABP5 standards, reagent A, reagent B, washing buffer, enzyme substrate, and stopping solution) was used to determine the impact of FABP5 siRNA treatment on FABP5 protein levels in hCMEC/D3 cells. Mock and FABP5 siRNA transfected hCMEC/D3 cells from T25 flasks were trypsinized and harvested by centrifugation. The cell pellet then underwent two freeze−thaw cycles followed by sonication for 30 s to release cellular proteins. Standards (recombinant hFABP5, 0.312, 0.625, 1.250 ng/mL in duplicates) and samples were loaded onto the ELISA plate and incubated for 2 h at 37 °C. Each well was then incubated with detection reagent A for 1 h at 37 °C and then thoroughly washed with washing buffer before reagent B was added for a

DOI: 10.1021/acs.molpharmaceut.5b00580
Mol. Pharmaceutics 2015, 12, 4375−4385

30 min incubation at 37 °C. Each well was thoroughly washed again prior to adding the enzyme substrate to start the colorimetric reaction. The reaction was ceased by adding the stopping solution after a 20 min incubation. Absorption at 450 nm was measured using an EnVision 2101 Multilabel reader (PerkinElmer, Boston, MA), and hCMEC/D3 concentration of FABP5 was determined by back-calculation to a calibration curve relating hFABP5 standard concentration to absorption at 450 nm.

hCMEC/D3 Cellular Uptake of ^{14}C-DHA and Impact of FABP5 siRNA. After hCMEC/D3 cells reached confluency, plates were placed in a THERMOstar (BMG Labtech, Ortenberg, Germany) at 37 °C shaking at 200 rpm for 5 min. Media was then removed and replaced with 0.5 mL of prewarmed uptake buffer (5% w/v HEPES in HBSS, pH 7.4) containing 0.5 μCi ^{14}C-DHA. An aliquot of spiking solution was collected from each well 20 s after addition to the wells to measure the initial concentration of ^{14}C-DHA to which the cells were exposed. At various time points (1, 1.5, 2, 5, 10, 15, and 20 min), ^{14}C-DHA uptake was ceased by removing the uptake buffer and rinsing the cells with ice-cold D-PBS three times. Cells were incubated with 0.25 mL of 1 M NaOH for 3 h at 37 °C, after which 0.1 mL of the cell lysate was removed and mixed with 0.05 mL of 2 M HCl. Spiking and cellular samples were thoroughly vortex-mixed with 2 mL of scintillation fluid (Ultima Gold Cocktail) and radioactivity determined in a PerkinElmer 2800TR liquid scintillation counter (Boston, MA). The remaining cell lysate was collected and total protein content determined using a Pierce BCA protein assay kit by comparison to known concentrations of bovine serum albumin (BSA) standard solutions prepared in 1 M NaOH. The mass of ^{14}C-DHA in cells was normalized by total protein count (mg), represented as cellular uptake (mL/mg) calculated using eq 3:

$$\text{Cellular uptake (mL/mg)} = \frac{^{14}\text{C} - \text{DHA in cellular lysate}\left(\frac{\text{dpm}}{\text{mg}}\right)}{^{14}\text{C} - \text{DHA in spiking solution}\left(\frac{\text{dpm}}{\text{mL}}\right)} \quad (3)$$

Identification of FABP5 in Murine Microvessels. Male Swiss Outbred mice were obtained from Monash Animal Research Platform, Monash University. All animal experiments were approved by the Monash Institute of Pharmaceutical Sciences Animal Ethics Committee and performed in accordance with the National Health and Medical Research Council guidelines for the care and use of animals for scientific purposes. The process of isolating microvessels was similar to that previously described.[22] All steps were conducted at 4 °C. Mice (n = 8/isolation) were anesthetized by isoflurane inhalation and decapitated. Mouse brains were immediately removed and placed in ice-cold microvessel buffer (pH 7.4) containing (in mM) 15 HEPES, 147 NaCl, 4 KCl, 3 $CaCl_2$, 1.2 $MgCl_2$, 5 glucose, and 0.5% w/v BSA. The cortex was separated from the cerebellum, meninges, brain stem, and large superficial blood vessels and homogenized in microvessel buffer with a Dounce homogenizer (Tissue Grinder, Potter-ELV, Millville, NJ) with 20 up-and-down manual strokes. The resulting homogenate was centrifuged at 1000g for 10 min. The pellet obtained at this step was suspended in 17% w/v dextran (70 kDa) and centrifuged for 90 min at 3900g. The supernatant containing the myelin layer was carefully removed, and the resulting pellet was suspended in microvessel buffer. The suspension was passed through a 100 μm nylon mesh filter to remove large blood vessels, and microvessels were trapped using a 20 μm mesh filter. The microvessels retained on the 20 μm mesh filter were collected by rinsing the filter with BSA-deficient microvessel buffer and centrifuging at 1000g for 40 min. The pellet was resuspended in HEPES (pH 7.4) and stored at −80 °C until required for protein analysis.

On the day of FABP5 identification, the isolated microvessels were incubated in lysis buffer (pH 7.4) containing 150 mM NaCl, 50 mM Tris-HCl, 0.5% v/v Triton X-100, 0.5% w/v sodium deoxycholate, and the Complete protease inhibitor cocktail at 4 °C for 45 min. The protein was separated from the microvessel debris by centrifuging in a mini-centrifuge (Eppendorf) at 12 100g for 1 min. The total protein concentration was determined using a Pierce BCA protein assay by comparison to known concentrations of BSA standards prepared in lysis buffer. A 15% polyacrylamide gel was loaded with 3.5 μg of total protein and Western blot analysis as detailed earlier for hFABP5 characterization.

Optimisation of *in Situ* Transcardiac Perfusion Technique. The *in situ* transcardiac perfusion technique was optimized in C57BL6/J male mice (6−8 weeks of age, 20−30 g, n = 3−5 for each data point presented). This technique has been employed previously in mice by Banks et al.,[23] where the perfusion was performed at 2 mL/min and BSA included in the perfusate. BSA is important for maintenance of cerebral vascular pressure, as it increases the viscosity of the perfusion fluid and hence the vessel pressure according to Poiseuille's law.[24] However, BSA may bind to ^{14}C-DHA, minimizing the free fraction and rate of transfer of ^{14}C-DHA across the BBB using the *in situ* transcardiac perfusion technique, which should be avoided in this study as the intention is to demonstrate any functional role of FABP5 at the BBB by comparing ^{14}C-DHA transport in FABP5$^{+/+}$ and FABP5$^{-/-}$ mice. As such, BSA was removed from the perfusion fluid, and this necessitated an increase in the flow rate to maintain perfusion pressure. The potential effect of the increase in flow rate was measured by assessing the brain uptake of ^{3}H-diazepam, the brain uptake of which is blood-flow dependent and used as a marker of cerebral perfusion.[25] Once an appropriate flow rate was determined, the structural integrity of the BBB paracellular route was assessed using ^{14}C-sucrose, and the functional integrity was monitored using ^{14}C-glucose ± 0.5 mM phloretin, a specific glucose transporter-1 (GLUT-1) inhibitor. For all experiments, the perfusion fluid used was Krebs carbonate-buffered physiologic saline (KBR) containing (in mM) 128 NaCl, 4.2 KCl, 1.5 $CaCl_2$, 0.9 $MgSO_4$, 24 $NaHCO_3$, 2.4 NaH_2PO_4, and 9.0 glucose. The solution was gassed with 95%O_2/5%CO_2, adjusted to pH 7.4, and warmed to 37 °C prior to each perfusion. The *in situ* transcardiac perfusion was performed as previously described.[22] Briefly, the mice were first anesthetized with an intraperitoneal injection of ketamine (133 mg/kg) and xylazine (10 mg/kg). Once anesthetized, the left and right jugular veins were isolated, and the thorax was opened to expose the heart. The descending thoracic aorta was clamped, followed by severing of both jugular veins, and perfusion fluid was infused into the left ventricle of the heart. The perfusion rate was controlled by a Harvard infusion pump (Harvard Apparatus, Holliston, MA). All perfusions were terminated by decapitating the animal, and the whole brain was harvested. Brain samples were digested in 2 mL of Solvable at 50 °C overnight and neutralized with 30% (v/v) hydrogen peroxide before 10 mL of Ultima Gold scintillation cocktail was added.

DOI: 10.1021/acs.molpharmaceut.5b00580
Mol. Pharmaceutics 2015, 12, 4375−4385

Two-hundred microliters of perfusate was also mixed with 2 mL of Ultima Gold scintillation cocktail. ^{14}C and ^{3}H radioactivity was then determined using the PerkinElmer 2800TR liquid scintillation analyzer. The apparent tissue distribution volume of the probe compound (B:P, mL/g) was calculated using Q_{brain}/C_p normalized by brain weight (g), where Q_{brain} is the radioactivity in the brain (DPM/g) (radioactivity from the vascular volume subtracted), and C_p is the radioactivity per mL of perfusate (DPM/mL). The vascular volume ($V_{vascular}$, mL/g) was estimated using ^{14}C-sucrose by $Q_{sucrose}/C_{sucrose}$ where $Q_{sucrose}$ is the radioactivity (DPM) of sucrose in the brain (DPM/g), and $C_{sucrose}$ is the radioactivity in perfusate (DPM/mL). The BBB transfer coefficient for unidirectional uptake of the probe compound from the perfusion fluid into brain (K_{in}; mL/g/s) was calculated by dividing B:P by the perfusion duration (s).

BBB Transport of ^{14}C-DHA and the Impact of FABP5 Deletion. By using the optimized flow rate (10 mL/min), the perfusion of ^{14}C-DHA was measured at different times to assess the linearity of DHA transport. This was necessary to allow appropriate choice of a time point at which to assess ^{14}C-DHA transport in FABP5$^{+/+}$ and FABP5$^{-/-}$ mice. Following perfusion, the brain and perfusate were quantified for ^{14}C-DHA concentration by liquid scintillation counting as detailed earlier. FABP5$^{-/-}$ mice on C57BL6/J background were crossed with C57BL6/J to produce heterozygous offspring, which were inbred to produce FABP5$^{-/-}$ and litter mate FABP5$^{+/+}$ mice. All mice were genotyped for the presence or absence FABP5 gene by Transnetyx (Cordova, TN). Given that the conditions eventually used for assessing ^{14}C-DHA transport in FABP5$^{+/+}$ and FABP$^{-/-}$ mice were optimized in C57BL6/J mice, the BBB transport of the marker compound ^{3}H-diazepam was assessed in both C57BL6/J mice and FABP5$^{+/+}$ and FABP5$^{-/-}$ mice (to ensure no strain differences in BBB permeability). After a 1 min blank preperfusion at 10 mL/min, ^{3}H-diazepam was perfused for 1 min at 10 mL/min, after which brain and perfusate were quantified by liquid scintillation counting. A comparison of BBB transport of ^{3}H-diazepam in FABP5$^{+/+}$ and FABP5$^{-/-}$ mice would also provide insight into whether the effect of FABP5 deletion could discriminate between a high affinity FABP5 substrate (i.e., ^{14}C-DHA) and ^{3}H-diazepam, which we have demonstrated to exhibit very low affinity for FABP5.[15]

Statistical Analysis of Data. All data were expressed as mean ± SEM. The comparisons between experimental and control groups were evaluated by Student's unpaired t tests. Comparisons among more than two groups were evaluated by a one-way ANOVA followed by a Tukey or Dunnett post hoc test where appropriate. Values showing $p < 0.05$ were considered statistically significant unless otherwise indicated in the text.

RESULTS

Purification and Characterization of hFABP5 from *E. coli*. hFABP5 was purified from cytosolic extracts of *E. coli* harboring the pET-28a(+)-hFABP5 plasmid. The homogeneity of the hFABP5 was ascertained by SDS-PAGE followed by Coomassie blue protein staining. As shown in Figure 1, panel A, a single polypeptide band with a molecular weight of 15 kDa was observed. In addition, hFABP5 was recognized by a rabbit anti-FABP5 antibody at the correct molecular weight (Figure 1B). The molecular weight of the purified protein was measured to be 15 429 ± 1.08 Da using mass spectrometry (ESIprot) (Supporting Information, SI-1).

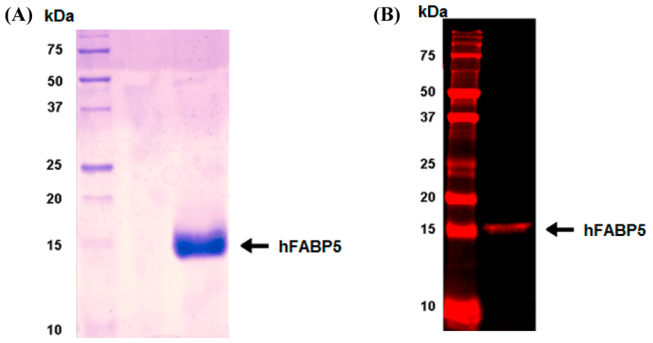

Figure 1. (A) Coomassie blue stain and (B) Western blot of purified recombinant hFABP5 following application of 10 and 0.25 μg of total protein, respectively. A single band was detected in both cases at 15 kDa, which was in agreement with the molecular weight of hFABP5.

Recombinant hFABP5 Binds to DHA with High Affinity. Shown in Figure 2, panel A is the isotherm generated from a blank titration to measure background heat of dilution, where hFABP5 was injected into the sample cell containing blank storage buffer. The background heat of dilution was approximately 0.03 μcal/s. The calorimetric isotherm of hFABP5 titration into DHA is shown in Figure 2, panel B. After 12 injections, the signal detected was similar to the blank titration, and therefore the peaks after the 12th injection were considered to be resulting from the heat of dilution. The background heat of dilution was therefore subtracted from the isotherm for data analysis. The recombinant hFABP5 bound to DHA with an equilibrium dissociation constant (K_D) of 155 ± 8 nM (n = 15), and the binding stoichiometry (N) was 1.00 ± 0.02 (n = 15), confirming that one molecule of hFABP5 binds to one molecule of DHA.

FABP5 siRNA Treatment Decreases hCMEC/D3 Cell Uptake of ^{14}C-DHA. The mRNA expression of FABP5 in hCMEC/D3 cells was reduced by 53.2 ± 7.1% following treatment with 5 nM siRNA for 96 h as assessed by qPCR (Figure 3A). This was consistent with a 44.8 ± 13.7% reduction in FABP5 protein expression as assessed by ELISA (Figure 3B). The cell morphology was not affected by the 96-h exposure to 5 nM siRNA (Figure 3C) when compared to untreated cells (Figure 3D). In contrast, toxic effects were observed at higher concentrations of siRNA (25 nM for 24 h) (Figure 3E). Time-dependent uptake studies were then conducted to determine an appropriate time frame to assess the impact of FABP5 siRNA treatment on ^{14}C-DHA uptake. The hCMEC/D3 cell uptake of ^{14}C-DHA increased in a linear manner over 2 min and appeared to plateau between 2 and 5 min (Figure 4). The impact of FABP5 siRNA on ^{14}C-DHA uptake was therefore assessed at the 2 min time point. Treating cells with 5 nM siRNA for 96 h led to a 14.1 ± 2.7% reduction in ^{14}C-DHA uptake ($p < 0.001$) over this 2 min period (Figure 5).

FABP5 Is Expressed at the Murine BBB. Following isolation of murine microvessels, Western blotting confirmed the expression of mFABP5 (Figure 6), suggesting that further studies manipulating FABP5 expression at the murine BBB could provide insight into any functional role of FABP5 *in vivo*.

An *in Situ* Transcardiac Perfusion Model in Mice for Assessing BBB Transport of ^{14}C-DHA. Diazepam transport is flow-limited; it is commonly used to estimate vascular tissue flow when the vascular perfusion fluid contains no proteins or blood cells.[21] With the BSA-deficient perfusion fluid, a flow rate of 5 mL/min for 2 min resulted in a K_{in} for ^{3}H-diazepam of

DOI: 10.1021/acs.molpharmaceut.5b00580
Mol. Pharmaceutics 2015, 12, 4375−4385

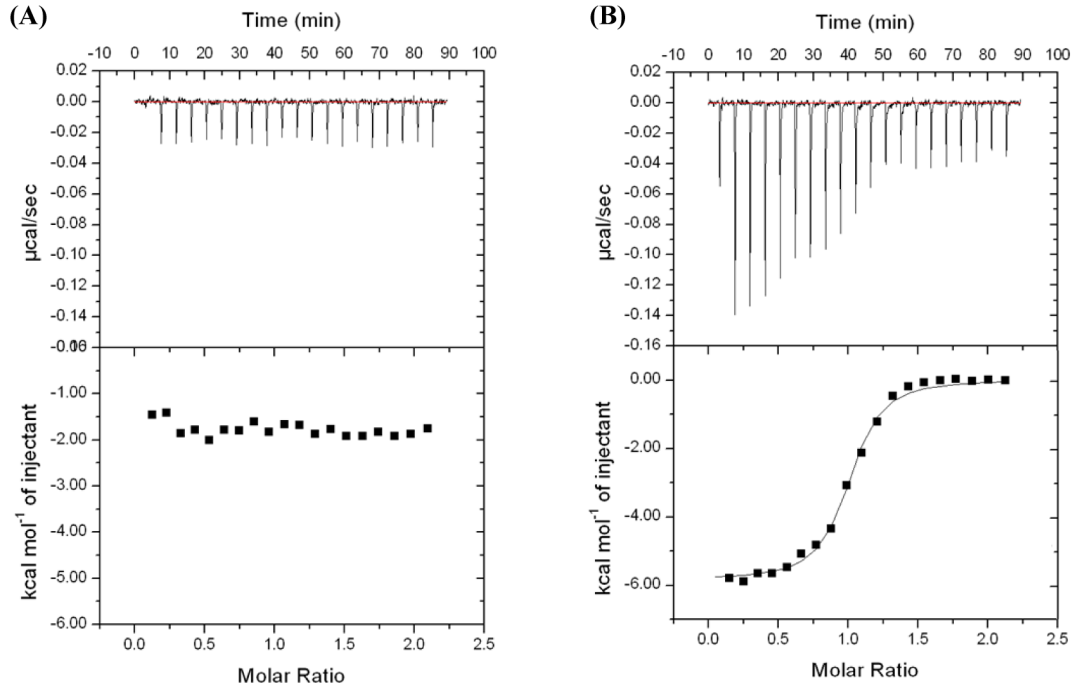

Figure 2. Binding isotherm of DHA to hFABP5 at 25 °C assessed using ITC. The processed data are shown as a plot of the heat generated per s (μcal/s) from injecting a hFABP5 solution into a DHA solution versus time (min), with each peak representing an injection and the integrated area representing the total energy generated from each injection (upper panel). For the lower panel, the total energy generated from each injection (kcal) as a function of total DHA injected (mol) is plotted against the molar ratio between hFABP5 and DHA. Diagram A is a representative blank titration of hFABP5 into storage buffer; B is a representative titration curve of hFABP5 into DHA. K_D and N were calculated as 155 ± 8 nM and 1.02 ± 0.02 (mean ± SEM, n = 15), respectively.

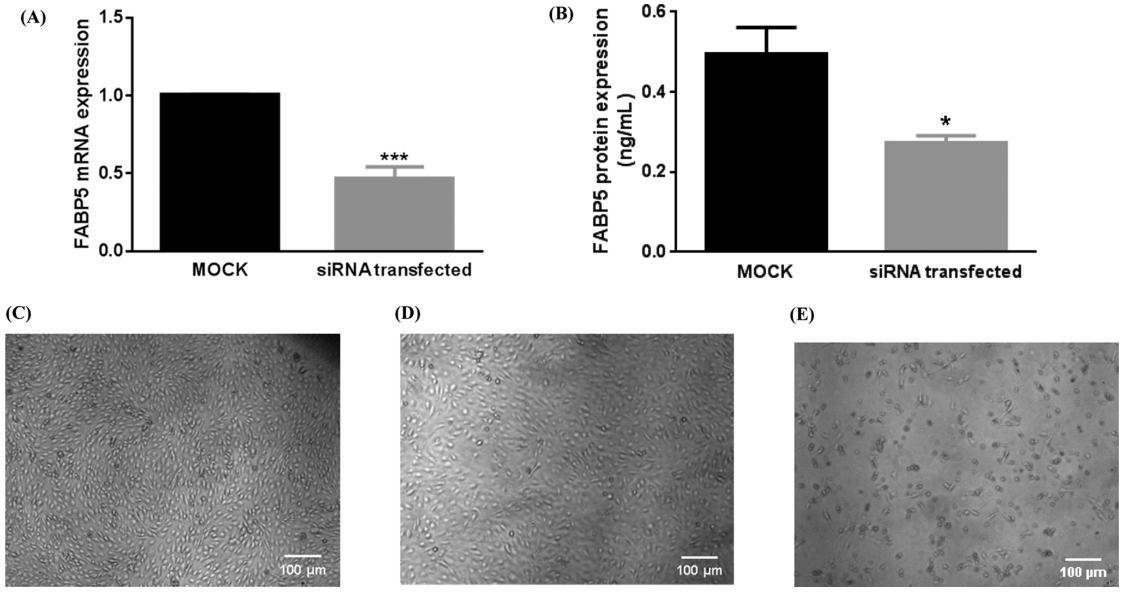

Figure 3. FABP5 expression at (A) mRNA and (B) protein level in mock cells (hCMEC/D3 treated with transfection reagent only) and hCMEC/D3 transfected with 5 nM FABP5 siRNA for 96 h. Data are presented as mean ± SEM, n = 4 with ∗ (p < 0.05) and ∗∗∗ (p < 0.001) determined using an independent sample t test. (C) Untreated hCMEC/D3 cells appeared similar in morphology to (D) hCMEC/D3 cells treated with 5 nM siRNA for 96 h, whereas (E) hCMEC/D3 cells treated with 25 nM siRNA for 24 h appeared to be grossly affected morphologically.

0.005 ± 0.001 mL/s/g (Figure 7A). Increasing the flow rate to 10 mL/min improved the ^{3}H-diazepam K_{in} to 0.017 ± 0.003 mL/s/g, more in line with previous reports[20] using the traditional internal carotid artery perfusion method in mice. On the basis of these findings and considering the physiological cardiac output in small mammals,[27] a flow rate of 10 mL/min was considered appropriate. Given that ^{14}C-DHA perfusion studies were also likely to occur over shorter periods of time (usually <60 s), and possibly with preperfusion with blank buffer (to remove any residual blood in the perfusate), the K_{in} of ^{3}H-diazepam was also measured under such conditions to ensure such modifications would not impact on cerebrovascular pressure. When perfused for 1 min at 10 mL/min, the K_{in} of ^{3}H-diazepam (0.020 ± 0.003 mL/s/g) was not significantly

DOI: 10.1021/acs.molpharmaceut.5b00580
Mol. Pharmaceutics 2015, 12, 4375−4385

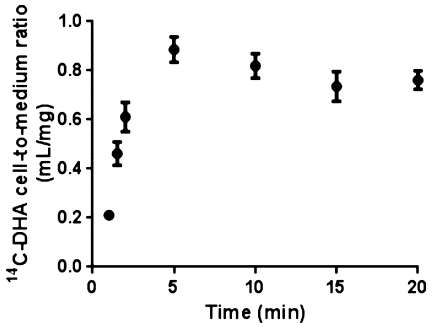

Figure 4. Time-dependent hCMEC/D3 cellular uptake of ^{14}C-DHA uptake after application of 0.5 μCi ^{14}C-DHA to each well. The apparent volume of ^{14}C-DHA uptake into the cells was normalized by total cellular protein (mL/mg). Data are presented as mean ± SEM (n = 3−15). The error bar for t = 1 min is not visible due to the minimal error observed in the data at this time point.

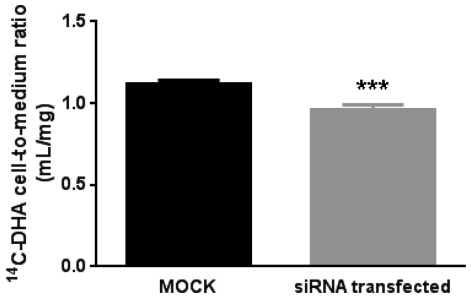

Figure 5. Impact of 96 h FABP5 siRNA or transfection reagent (MOCK) treatment on hCMEC/D3 cellular uptake of ^{14}C-DHA over 2 min. The cellular ^{14}C-DHA uptake (mL) was normalized by the total cellular protein (mg) and expressed as cell-to-medium ratio. Data are presented as mean ± SEM (n = 13), and *** indicates a significant (p < 0.001) difference between siRNA and transfection reagent alone (MOCK) using an unpaired student t test.

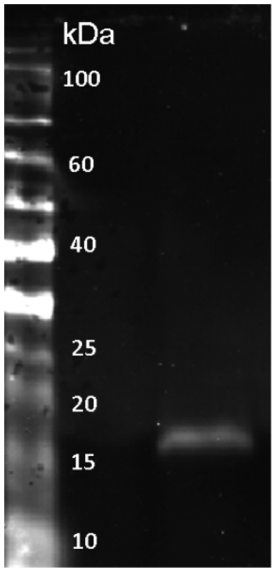

Figure 6. Identification of FABP5 in brain microvessels isolated from Swiss Outbred mice using Western Blot. A single band at 15 kDa was detected following application of 3.5 μg of total protein extract.

different to that obtained after a 2 min perfusion (Figure 7A). Furthermore, the inclusion of a 1 min preperfusion at 10 mL/min (with blank buffer) followed by a 1 min perfusion of ^{3}H-diazepam at 10 mL/min resulted in a K_{in} value of 0.018 ± 0.001 mL/s/g, which was not significantly different to K_{in} values determined in the absence of the preperfusion. The physical integrity of the vasculature was also maintained using this higher perfusion rate (10 mL/min over 2 min) as measured by ^{14}C-sucrose with a B:P ratio of 0.007 ± 0.001 mL/g. Furthermore, the functional integrity of the BBB (in terms of active transport) was maintained under these conditions, as assessed with ^{14}C-glucose (Figure 7B). Preperfusing mice for 1 min with 0.5 mM phloretin (specific GLUT-1 inhibitor) followed by a 1 min coperfusion with phloretin resulted in an 85.9 ± 3.9% reduction in ^{14}C-glucose transport across the BBB (Figure 7B).

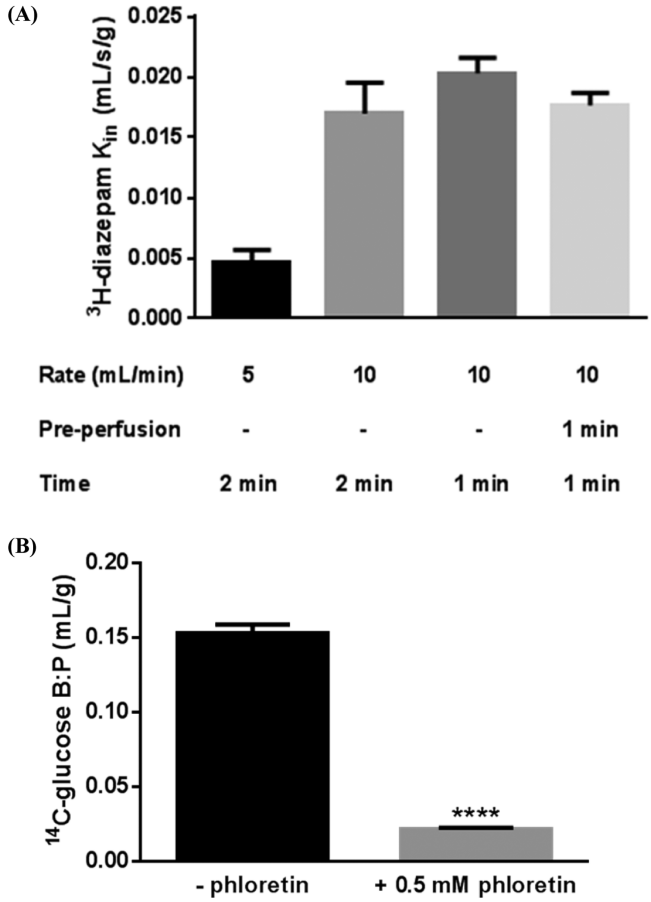

Figure 7. (A) K_{in} of ^{3}H-diazepam following *in situ* transcardiac perfusion in male C57BL6/J mice under various perfusion conditions (altered perfusion rate, incorporation of a preperfusion and time of perfusion). (B) ^{14}C-glucose BBB transport (expressed as B:P ratio) following perfusion with or without 0.5 mM phloretin to male C57BL6/J mice. Data are presented as mean ± SEM of 3−4 animals; **** indicates a significant difference with p < 0.0001 (unpaired two-sided t test).

^{14}C-DHA was perfused to mice in BSA-deficient KBR at 10 mL/min (over 20, 40, and 60 s), and this resulted in linear BBB transport over 60 s with a K_{in} of 0.0052 mL/s/g (Figure 8). Therefore, a 60 s period was determined to be the suitable for future ^{14}C-DHA perfusions. Under these conditions the ^{14}C-DHA B:P ratio from a 1 min perfusion at 10 mL/min (0.44 ± 0.08 mL/g) was lower than that reported in the literature (2.88 ± 0.18 mL/g),[10] which was considered to result from binding to residual plasma components in the perfusion fluid. Therefore, a preperfusion step (blank KBR) was incorporated

DOI: 10.1021/acs.molpharmaceut.5b00580
Mol. Pharmaceutics 2015, 12, 4375−4385

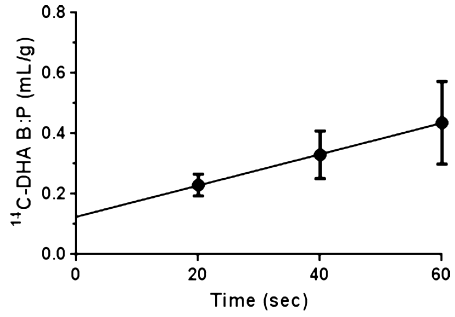

Figure 8. BBB transport of ^{14}C-DHA expressed as a B:P ratio following perfusion (10 mL/min) in male C57BL6/J mice over 20, 40, and 60 s, with a linear regression of the mean B:P ratios yielding a K_{in} of 0.0052 mL/s/g (r^2 = 0.9997). Data are presented as mean ± SEM (n = 3–4).

prior to perfusion with ^{14}C-DHA. With this preperfusion step, a four-fold increase in the B:P ratio of ^{14}C-DHA was observed (1.78 ± 0.10 mL/g), more in line with that reported in the literature.

FABP5 Deletion Reduces BBB Transport of ^{14}C-DHA. Using the optimized conditions identified earlier, the BBB transport of ^{14}C-DHA was assessed in FABP5$^{-/-}$ mice and their litter mate FABP5$^{+/+}$ controls. As shown in Figure 9, panel A, the B:P ratio of ^{14}C-DHA in FABP5$^{-/-}$ mice was 36.7 ± 12.4% lower than that determined in FABP5$^{+/+}$ mice. Importantly, there was no significant difference in the B:P ratio of ^{3}H-diazepam between FABP5$^{+/+}$ and FABP5$^{-/-}$ mice, nor was there a significant difference between the B:P ratio of ^{3}H-diazepam between C57BL/6 mice and the FABP5 wild-type strain (Figure 9B).

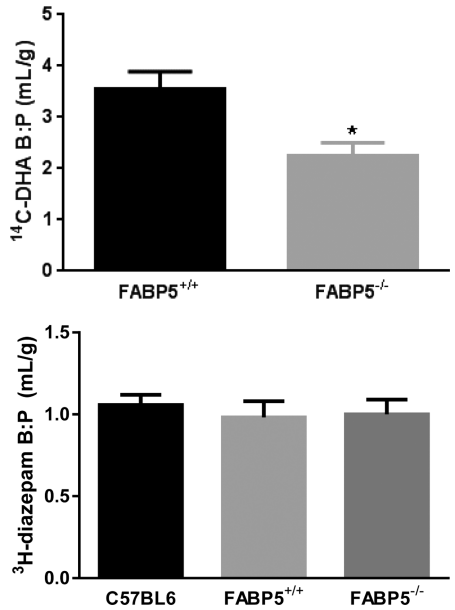

Figure 9. (A) B:P ratio of ^{14}C-DHA following *in situ* transcardiac perfusion in FABP5$^{+/+}$ and FABP5$^{-/-}$ C57BL6/J mice with 1 min blank preperfusion and 1 min perfusion with ^{14}C-DHA at 10 mL/min. FABP5$^{-/-}$ mice demonstrated a lower rate of DHA BBB transport, with * indicating a significant difference (p < 0.05) (unpaired two-sided student t test). (B) B:P ratio of ^{3}H-diazepam following *in situ* transcardiac perfusion in C57BL6/J mice, FABP5$^{+/+}$ mice and FABP5$^{-/-}$ mice (derived on a C57BL6/J strain) with 1 min blank preperfusion and 1 min perfusion with ^{3}H-diazepam at 10 mL/min. No statistical significance was identified using a one-way ANOVA. Data are presented as mean ± SEM of 3–5 animals.

DISCUSSION

In some neurological diseases, including Alzheimer's disease, DHA levels in the brain are reduced.[28] Since DHA is an essential fatty acid not produced by the brain, brain DHA levels are maintained by transport of plasma DHA across the BBB. Therefore, approaches that enhance BBB transport of DHA have been considered as a potential therapeutic approach to restore CNS access of DHA in conditions where DHA brain levels are augmented.[28] Regardless of the passive or active nature by which DHA permeates the luminal membrane of the brain endothelial cell, it is likely that an intracellular carrier protein is required to facilitate cytosolic trafficking of DHA across the brain endothelial cell, given its poor aqueous solubility. The purpose of this study, therefore, was to assess the role of the intracellular carrier protein FABP5 in the brain endothelial cell uptake of DHA *in vitro* and BBB transport of DHA *in vivo*.

We have recently confirmed the gene and protein expression of FABP3, 4, and 5 at the human BBB, with FABP5 appearing to exhibit the highest expression in hCMEC/D3 cells.[15] This finding is consistent with a previous study that reported the expression of FABP5 in primary human brain endothelial cells and implicated FABP5 in the transport of palmitic, oleic, and linoleic acid across primary brain endothelial cells.[8] This led us to investigate whether FABP5 contributed to DHA transport across the BBB. To the best of our knowledge, this is the first study to highlight the role of FABPs in the brain access of any PUFA *in vivo*. hFABP5 was expressed in *E. coli* and purified to homogeneity. DHA binding to rodent FABP5 has been examined previously via displacement of 1-anilinonaphthalene-8-sulfonic acid (ANS) and found to be slightly higher than what we have determined with DHA binding to rodent FABP5 reported as 422 nM.[29] This discrepancy could not only arise from the differences in techniques used to probe binding to FABP5, but also could be a result of species difference in binding to DHA, as has been reported previously for oleic acid.[14] DHA exhibits different binding affinities across FABPs. For example, the binding affinity of DHA to FABP7 has been found to be 53.4 nM, whereas the affinity for FABP3 is lower (4100 nM)[30] measured by ITC. Our studies have demonstrated that the affinity of FABP5 to DHA ranges between that observed for FABP3 and FABP7, and is of a high affinity nature, as would be expected for a fatty acid.

Having demonstrated that FABP5 binds to DHA, we subsequently investigated whether FABP5 had any functional role in the brain endothelial cell uptake of ^{14}C-DHA using hCMEC/D3 cells. hCMEC/D3 cells maintain stable growth and endothelial marker characteristics, at least until passage 35.[31] Although tight junction proteins are expressed in this cell line, the transendothelial electrical resistance of hCMEC/D3 monolayers often does not exceed 1000 Ω cm^2, which is below that reported for an intact BBB *in vivo*.[32] For this reason, we performed uptake studies in hCMEC/D3 cells, rather than permeability studies across the cell monolayer, to avoid confounding issues associated with the leakiness of the monolayer. The uptake of ^{14}C-DHA into hCMEC/D3 cells was rapid and linear between 0 and 2 min and appeared to reach a plateau between 2 and 5 min. It was important to determine the linear portion of ^{14}C-DHA uptake as this would then govern at what time point subsequent studies would be

DOI: 10.1021/acs.molpharmaceut.5b00580
Mol. Pharmaceutics 2015, 12, 4375–4385

undertaken in cells treated with FABP5 siRNA. The extent of down-regulation using FABP5 siRNA was similar to that previously reported in primary human brain endothelial cells.[8] This 45−53% reduction in FABP5 was associated with a small but statistically significant (14%) reduction in the uptake of ^{14}C-DHA into hCMEC/D3 cells. It is likely that intracellular FABP5 assists in the dissociation of DHA from the luminal membrane, given the low aqueous solubility of this PUFA. The reduction in FABP5 protein in the aqueous cytosol likely decreases the rate of DHA dissociation from the luminal membrane, leading to reduced DHA entry into the cells. Surprisingly, despite an almost halving of FABP5 protein expression, the uptake of ^{14}C-DHA, which has nM affinity for FABP5, was not decreased to a similar extent as observed with the reduction in protein expression. This is likely due to the fact that FABP5 is so abundant that a 45% reduction in its expression may not have a dramatic impact on its cellular uptake function. Furthermore, silencing of FABP5 in hCMEC/D3 cells may be associated with increased expression of other proteins that are involved in fatty acid uptake, albeit this was not investigated in this study. Since we have recently demonstrated that FABP3 and FABP4 are also expressed at the BBB,[15] there could be a compensatory up-regulation of these two FABPs, which could attenuate the expected effect of FABP5 down-regulation on DHA uptake. It should also be noted that mock cells appear to have higher ^{14}C-DHA uptake (cell-to-medium ratio of approximately 1.1 in Figure 5) relative to nontransfected hCMEC/D3 cells (cell-to-medium ratio of approximately 0.6 at 2 min in Figure 4), suggesting that the transfection reagent might affect the cell permeability to ^{14}C-DHA. Regardless of this potential effect of transfection reagent on hCMEC/D3 permeability on ^{14}C-DHA, it is evident that siRNA treated hCMEC/D3 still exhibited a lower ^{14}C-DHA uptake compared to the mock cells, implicating a functional involvement of FABP5 in ^{14}C-DHA brain endothelial cell uptake.

To avoid the potential limitations of *in vitro* cell uptake studies, the impact of FABP5 deletion on the BBB transport of ^{14}C-DHA was then assessed using an *in situ* transcardiac perfusion technique in FABP5$^{+/+}$ and FABP5$^{-/-}$ mice. Prior to assessing DHA transport *in situ*, it was necessary to optimize the transcardiac perfusion technique in mice. As previously described, the mechanism by which DHA is transported across the BBB may involve both passive diffusion and active transport.[8−10] Therefore, perfusion conditions that compromise neither passive diffusion nor active transport were required. The *in situ* transcardiac perfusion technique was originally modified from the mouse internal carotid artery perfusion method[25] by Banks et al.[23] In this original internal carotid artery perfusion technique, a perfusion rate of 2 or 2.5 mL/min was employed. The transcardiac technique modified by Banks simplified the surgical procedure as the transcardiac perfusion technique removes the requirement to isolate the internal carotid artery. However, as the transcardiac perfusion technique also perfuses noncerebral regions, an adequate cerebral vascular pressure was maintained by the addition of BSA in the perfusate.[18] However, as DHA binds to BSA, and could hinder free DHA access to the BBB, with the purpose of this study being to assess the impact of FABP5 on BBB transport of DHA, it was considered necessary to measure BBB transport characteristics of ^{14}C-DHA and impact of FABP5 deletion in the absence of confounding factors such as plasma protein binding. It should be noted that, while this does not represent the typical *in vivo* situation (as plasma contains proteins and lipoproteins to which DHA binds), the *in situ* transcardiac perfusion technique (in the absence of plasma proteins) allows for more detailed evaluation of BBB transport processes.

However, to maintain cerebral vascular pressure, in the absence of BSA in the perfusion fluid, the flow rate had to be increased so as to maintain an appropriate cerebral vascular pressure. Maintenance of cerebral vascular pressure is important, as it affects the internal lateral bilayer pressure and subsequently influences the rate of diffusion of compounds across the BBB.[33] The K_{in} of diazepam was assessed at 5 and 10 mL/min to determine whether the increase in perfusion rate was sufficient to achieve appropriate passive permeability. At 10 mL/min, but not 5 mL/min, perfusion of ^{3}H-diazepam over 1−2 min resulted in a K_{in} value more in line with that previously reported using the internal carotid artery perfusion method in mice.[25] It has been previously demonstrated in small mammals,[26] the cardiac output (mL/min) can be calculated by 0·762(body weight in gram)$^{0.776}$. Given that the body weight of the animals used in this study was 25−30 g (resulting in a cardiac output of 9−11 mL/min), the perfusion rate of 10 mL/min used in this study was considered appropriate for maintenance of cerebral vascular pressure. While the K_{in} of diazepam was more in line with the literature using this flow rate of 10 mL/min (in the absence of BSA), it was important to ensure the structural integrity of the BBB also remained intact. ^{14}C-sucrose was used as a marker of the cerebral microvascular volume as it does not cross the BBB during brief periods of perfusion, and ^{14}C-glucose was used as a marker of functional integrity of the GLUT-1 transporter. Under the conditions used here, the cerebral microvascular volume was found to be 0.007 ± 0.001 mL/g, similar to that previously reported in mice using the internal carotid artery perfusion technique.[34] Furthermore, the B:P ratio of ^{14}C-glucose at 10 mL/min agreed with that reported in the literature[25] and was significantly decreased by the GLUT-1 inhibitor phloretin.[35] The data suggest that removal of BSA from the perfusion fluid and increasing the flow rate to 10 mL/min resulted in similar permeability characteristics of the BBB to that reported previously with the internal carotid artery perfusion technique.

Using these perfusion conditions, the B:P ratio of ^{14}C-DHA was much (6.5-fold) lower than that reported in the literature using the internal carotid *in situ* perfusion technique in mice (2.88 ± 0.18 mL/g).[10] We hypothesized that the lower K_{in} value may have resulted from ^{14}C-DHA binding to residual plasma proteins remaining in the vasculature (as there was no initial preperfusion prior to perfusing ^{14}C-DHA). To overcome this, a preperfusion step was therefore included in the protocol to remove residual plasma components. This resulted in a four-fold increase in the B:P ratio of ^{14}C-DHA to values more similar to that reported using the internal carotid artery perfusion technique.[10] These optimized *in situ* transcardiac perfusion conditions were applied in FABP5$^{+/+}$ and FABP5$^{-/-}$ mice to investigate the impact of FABP5 deletion on the BBB transport of ^{14}C-DHA. The K_{in} of DHA was reduced by 37% in FABP5$^{-/-}$ mice, suggesting that FABP5 plays an important role in DHA BBB transport *in vivo*. In line with what we observed *in vitro*, it therefore appears that FABP5 facilitates the uptake of DHA into the brain endothelial cells and traffics it to the abluminal membrane, where it is available for entry into the brain parenchyma. To our knowledge, this is the first study that demonstrates an intracellular carrier protein is involved in the BBB transport and CNS delivery of an endogenous molecule *in*

DOI: 10.1021/acs.molpharmaceut.5b00580
Mol. Pharmaceutics 2015, 12, 4375−4385

vivo. Importantly, we demonstrated that FABP5 deletion had no impact on the BBB transport of ^{3}H-diazepam, a molecule that has a substantially lower affinity for FABP5 relative to DHA (diazepam has a K_i of 325 μM to hFABP5 using a fluorescence displacement assay[15] relative to DHA, which we demonstrate in this study has a K_D of 155 nM using ITC). These findings suggest that the effect of FABP5 at the BBB is specific for high affinity substrates, potentially impacting on the CNS access of drugs, which also have high affinity for this intracellular protein. Whether FABP5, or indeed other FABPs present at the BBB, exhibit a similar role in trafficking of other endogenous molecules, and possibly other exogenous molecules, into the CNS remains unknown.

Interestingly, the reduction in BBB transport of ^{14}C-DHA observed in FABP5$^{-/-}$ mice was more evident than that observed in hCMEC/D3 cells following silencing with FABP5 siRNA. We hypothesize that the complete knock out of FABP5 had a more dramatic impact on ^{14}C-DHA transport, when compared to the approximate 50% knockdown of FABP5 observed in hCMEC/D3 cells, given the high concentration of FABP5 present in the brain microvascular endothelial cells. It should also be noted that the deletion of FABP5 in the current studies did not result in as dramatic an effect as deletion of the membrane transporter Mfsd2a, the deletion of which resulted in a 90% reduction in the brain uptake of ^{14}C-LPC-DHA. Clearly, Mfsd2a is important in the BBB transport of DHA; however, we demonstrate here that FABP5 is also a key contributor to the trafficking of DHA across the BBB. Given that FABP5 deletion was associated with a significant reduction in BBB transport of DHA, it is likely that this would result in attenuated endogenous DHA levels and cognitive dysfunction, which is the subject of further studies in our laboratory. In addition, given that FABP3 and FABP4 are expressed at the human BBB, the impact of deleting each of the genes encoding for these cytosolic proteins on DHA transport could be measured in the future to ascertain whether they also contribute to the CNS access of DHA.

In conclusion, the present study has demonstrated that FABP5 binds to DHA and facilitates DHA uptake and transport across the BBB. This study has highlighted the importance of an intracellular protein in brain DHA access, suggesting that in addition to membrane transporters, intracellular proteins play a crucial role in the transport of DHA across the BBB and possibly other fatty acids.

■ ASSOCIATED CONTENT

Supporting Information

The Supporting Information is available free of charge on the ACS Publications website at DOI: 10.1021/acs.molpharmaceut.5b00580.

Mass spectrum of purified recombinant hFABP5 identifying a species of molecular weight 15429 ± 1.08 Da (PDF)

■ AUTHOR INFORMATION

Corresponding Author

*Phone: +61 3 9903 9605. Fax: +61 3 9903 9583. E-mail: joseph.nicolazzo@monash.edu.

Notes

The authors declare no competing financial interest.

■ ACKNOWLEDGMENTS

The Judith Jane Mason and Harold Stannett Williams Memorial Foundation and The William Buckland Foundation are acknowledged for their financial support of this project.

■ ABBREVIATIONS

BBB, blood−brain barrier; DHA, docosahexaenoic acid; FABP, fatty acid-binding protein; FATP, fatty acid transport protein; hCMEC/D3, immortalized human brain microvascular endothelial cells; PUFA, polyunsaturated fatty acid

■ REFERENCES

(1) Yurko-Mauro, K.; Alexander, D. D.; Van Elswyk, M. E. Docosahexaenoic acid and adult memory: a systematic review and meta-analysis. *PLoS One* **2015**, *10* (3), e0120391.

(2) Lukiw, W. J.; Cui, J. G.; Marcheselli, V. L.; Bodker, M.; Botkjaer, A.; Gotlinger, K.; Serhan, C. N.; Bazan, N. G. A role for docosahexaenoic acid-derived neuroprotectin D1 in neural cell survival and Alzheimer disease. *J. Clin. Invest.* **2005**, *115* (10), 2774−83.

(3) Prasad, M. R.; Lovell, M. A.; Yatin, M.; Dhillon, H.; Markesbery, W. R. Regional membrane phospholipid alterations in Alzheimer's disease. *Neurochem. Res.* **1998**, *23* (1), 81−8.

(4) Soderberg, M.; Edlund, C.; Kristensson, K.; Dallner, G. Fatty acid composition of brain phospholipids in aging and in Alzheimer's disease. *Lipids* **1991**, *26* (6), 421−5.

(5) Rapoport, S. I.; Chang, M. C.; Spector, A. A. Delivery and turnover of plasma-derived essential PUFAs in mammalian brain. *J. Lipid. Res.* **2001**, *42* (5), 678−85.

(6) Rapoport, S. I.; Rao, J. S.; Igarashi, M. Brain metabolism of nutritionally essential polyunsaturated fatty acids depends on both the diet and the liver. *Prostaglandins, Leukotrienes Essent. Fatty Acids* **2007**, *77* (5−6), 251−61.

(7) Abbott, N. J.; Patabendige, A. A. K.; Dolman, D. E. M.; Yusof, S. R.; Begley, D. J. Structure and function of the blood−brain barrier. *Neurobiol. Dis.* **2010**, *37* (1), 13−25.

(8) Mitchell, R. W.; On, N. H.; Del Bigio, M. R.; Miller, D. W.; Hatch, G. M. Fatty acid transport protein expression in human brain and potential role in fatty acid transport across human brain microvessel endothelial cells. *J. Neurochem.* **2011**, *117* (4), 735−46.

(9) Nguyen, L. N.; Ma, D.; Shui, G.; Wong, P.; Cazenave-Gassiot, A.; Zhang, X.; Wenk, M. R.; Goh, E. L.; Silver, D. L. Mfsd2a is a transporter for the essential omega-3 fatty acid docosahexaenoic acid. *Nature* **2014**, *509* (7501), 503−6.

(10) Ouellet, M.; Emond, V.; Chen, C. T.; Julien, C.; Bourasset, F.; Oddo, S.; LaFerla, F.; Bazinet, R. P.; Calon, F. Diffusion of docosahexaenoic and eicosapentaenoic acids through the blood−brain barrier: An *in situ* cerebral perfusion study. *Neurochem. Int.* **2009**, *55* (7), 476−482.

(11) Larque, E.; Krauss-Etschmann, S.; Campoy, C.; Hartl, D.; Linde, J.; Klingler, M.; Demmelmair, H.; Cano, A.; Gil, A.; Bondy, B.; Koletzko, B. Docosahexaenoic acid supply in pregnancy affects placental expression of fatty acid transport proteins. *Am. J. Clin. Nutr.* **2006**, *84* (4), 853−61.

(12) Vorum, H.; Brodersen, R.; Kragh-Hansen, U.; Pedersen, A. O. Solubility of long-chain fatty acids in phosphate buffer at pH 7.4. *Biochim. Biophys. Acta, Lipids Lipid Metab.* **1992**, *1126*, 135−42.

(13) Weisiger, R. A. Mechanisms of intracellular fatty acid transport: role of cytoplasmic-binding proteins. *J. Mol. Neurosci.* **2007**, *33* (1), 42−4.

(14) Storch, J.; McDermott, L. Structural and functional analysis of fatty acid-binding proteins. *J. Lipid Res.* **2008**, *50* (Suppl), S126−31.

(15) Lee, G.; Kappler, K.; Porter, C. H.; Scanlon, M.; Nicolazzo, J. Fatty acid binding proteins expressed at the human blood−brain barrier bind drugs in an isoform-specific manner. *Pharm. Res.* **2015**, *32* (10), 3432−46.

(16) Richieri, G. V.; Ogata, R. T.; Zimmerman, A. W.; Veerkamp, J. H.; Kleinfeld, A. M. Fatty acid binding proteins from different tissues

DOI: 10.1021/acs.molpharmaceut.5b00580
Mol. Pharmaceutics 2015, 12, 4375−4385

show distinct patterns of fatty acid interactions. *Biochemistry* **2000**, *39* (24), 7197−204.
(17) Corsico, B.; Cistola, D. P.; Frieden, C.; Storch, J. The helical domain of intestinal fatty acid binding protein is critical for collisional transfer of fatty acids to phospholipid membranes. *Proc. Natl. Acad. Sci. U. S. A.* **1998**, *95* (21), 12174−8.
(18) Herr, F. M.; Aronson, J.; Storch, J. Role of portal region lysine residues in electrostatic interactions between heart fatty acid binding protein and phospholipid membranes. *Biochemistry* **1996**, *35* (4), 1296−303.
(19) Franchini, G. R.; Storch, J.; Corsico, B. The integrity of the alpha-helical domain of intestinal fatty acid binding protein is essential for the collision-mediated transfer of fatty acids to phospholipid membranes. *Biochim. Biophys. Acta, Mol. Cell Biol. Lipids* **2008**, *1781* (4), 192−9.
(20) Liou, H. L.; Storch, J. Role of surface lysine residues of adipocyte fatty acid-binding protein in fatty acid transfer to phospholipid vesicles. *Biochemistry* **2001**, *40* (21), 6475−85.
(21) Froger, A.; Hall, J. E. Transformation of plasmid DNA into *E. coli* using the heat shock method. *J. Visualized Exp.* **2007**, *6*, 253.
(22) Mehta, D. C.; Short, J. L.; Nicolazzo, J. A. Altered brain uptake of therapeutics in a triple transgenic mouse model of Alzheimer's disease. *Pharm. Res.* **2013**, *30* (11), 2868−79.
(23) Banks, W. A.; Niehoff, M. L.; Zalcman, S. S. Permeability of the mouse blood−brain barrier to murine interleukin-2: predominance of a saturable efflux system. *Brain, Behav., Immun.* **2004**, *18* (5), 434−42.
(24) Letcher, R. L.; Chien, S.; Pickering, T. G.; Sealey, J. E.; Laragh, J. H. Direct relationship between blood pressure and blood viscosity in normal and hypertensive subjects. Role of fibrinogen and concentration. *Am. J. Med.* **1981**, *70* (6), 1195−1202.
(25) Dagenais, C.; Rousselle, C.; Pollack, G. M.; Scherrmann, J. M. Development of an *in situ* mouse brain perfusion model and its application to mdr1a P-glycoprotein-deficient mice. *J. Cereb. Blood Flow Metab.* **2000**, *20* (2), 381−6.
(26) Takasato, Y.; Rapoport, S. I.; Smith, Q. R. An *in situ* brain perfusion technique to study cerebrovascular transport in the rat. *Am. J. Physiol.* **1984**, *247* (3 Pt 2), H484−93.
(27) White, L.; Haines, H.; Adams, T. Cardiac output related to body weight in small mammals. *Comp. Biochem. Physiol.* **1968**, *27* (2), 559−565.
(28) Pan, Y.; Khalil, H.; Nicolazzo, J. A. The impact of docosahexaenoic acid on Alzheimer's disease: is there a role of the blood−brain barrier? *Curr. Clin. Pharmacol.* **2015**, *10* (3), 222−41.
(29) Liu, J. W.; Almaguel, F. G.; Bu, L.; De Leon, D. D.; De Leon, M. Expression of E-FABP in PC12 cells increases neurite extension during differentiation: involvement of n-3 and n-6 fatty acids. *J. Neurochem.* **2008**, *106* (5), 2015−29.
(30) Balendiran, G. K.; Schnutgen, F.; Scapin, G.; Borchers, T.; Xhong, N.; Lim, K.; Godbout, R.; Spener, F.; Sacchettini, J. C. Crystal structure and thermodynamic analysis of human brain fatty acid-binding protein. *J. Biol. Chem.* **2000**, *275* (35), 27045−54.
(31) Weksler, B.; Romero, I.; Couraud, P.-O. The hCMEC/D3 cell line as a model of the human blood brain barrier. *Fluids Barriers CNS* **2013**, *10* (1), 16.
(32) Butt, A. M.; Jones, H. C.; Abbott, N. J. Electrical resistance across the blood−brain barrier in anaesthetized rats: a developmental study. *J. Physiol.* **1990**, *429*, 47−62.
(33) Fischer, H.; Gottschlich, R.; Seelig, A. Blood−brain barrier permeation: molecular parameters governing passive diffusion. *J. Membr. Biol.* **1998**, *165* (3), 201−11.
(34) Cattelotte, J.; Andre, P.; Ouellet, M.; Bourasset, F.; Scherrmann, J. M.; Cisternino, S. *In situ* mouse carotid perfusion model: glucose and cholesterol transport in the eye and brain. *J. Cereb. Blood Flow Metab.* **2008**, *28* (8), 1449−59.
(35) Afzal, I.; Cunningham, P.; Naftalin, R. J. Interactions of ATP, oestradiol, genistein and the anti-oestrogens, faslodex (ICI 182780) and tamoxifen, with the human erythrocyte glucose transporter, GLUT1. *Biochem. J.* **2002**, *365* (3), 707−719.

DOI: 10.1021/acs.molpharmaceut.5b00580
Mol. Pharmaceutics 2015, 12, 4375−4385